# Numerical Simulation of g-jitter Effects on Half Floating Zone Convection Under Microgravity Environment

Hao Tang, Z.M. Tang, W.R. Hu, G Chen, B Roux

# Numerical Simulation of g-jitter Effects on Half Floating Zone Convection Under Microgravity Environment

H. Tang, Z.M. Tang, W.R. Hu, G. Chen, and B. Roux

*The g-jitter effects on the thermocapillary convection in liquid bridge of floating half zone were studied by numerical simulation for unsteady and axi-symmetric model in the cylindrical coordinate system. The g-jitter field was given by a steady microgravity field in addition to an oscillatory low-gravity field, and the effects on the flow field, temperature distribution and free surface deformation were analyzed numerically.*

## 1 Introduction

Many programmes paid attention to measure the residual acceleration of micro- or low-gravity environment on board spacecraft in near earth orbit. Results of space experiments show that the residual acceleration or $g$-jitter may have serious influence on the experimental process. The properties and influence of residual gravity have been studied extensively in recent years (see, for example, the reviews [1, 2]). Many Russian scientists discussed the so-called thermovibrational convection by time-averaged method, which can only be applied to study the phenomena of high frequency $g$-jitters, see for example [3]. To study directly the response of a sinuous $g$-jitter field, the numerical simulation method for the complete problem should be used.

In addition to the real time measurements of the microgravity environment in the spacecraft, the theoretical estimation of $g$-jitter effects have been discussed. Usually, the numerical simulations have been applied to calculate the response of $g$-jitter field on a special process. The $g$-jitter field was often assumed in the numerical simulation to oscillate with a relative higher frequency, and then, the free surface or interface was assumed to be undeformable [4–6]. *Briskman* [4] discussed the problem about vibrational thermocapillary convection and stability. In his work, the system of equations and boundary conditions are formulated for high frequency approximation. Many studies concentrate especially to the process associated with crystal growth, and analyze the influence of a typical residual acceleration of spacecraft on the solidification [7, 8].

The ground-based experiments were performed to simulate the effect of $g$-jitter by fixing a system of half floating zone convection on a vibrating table [9–11]. Experimental results show that there are a steady component and an oscillatory component of the velocity field and the temperature field as response to the simulated $g$-jitter field in the frequency range from 0.1 Hz to 100 Hz, and the free surface is deformed obviously in the lower frequency range. In the present paper, the numerical simulation of unsteady Navier–Stokes equations was completed to study the nonlinear process of $g$-jitter effect on half floating zone convection including the deformation of free surface. The results may be applied to study not only the response to high frequency but also to low frequency $g$-jitter fields. The results of the present paper show that the flow will be retarded and the temperature gradient will be decreased in vibration environment.

## 2 Description of the Model

An axi-symmetric floating half zone is contained between two parallel coaxial circular rigid disks with $R_0$ in radius. The 10 cSt silicon oil liquid bridge is held between the disks by surface tension as shown in fig. 1. The free surface of the liquid bridge is a gas liquid interface and is deformable. Each disk is maintained at a constant temperature and the temperature at the upper rod is higher. The residual acceleration is parallel to the cylinder axis ($z$-axis), the axi-symmetric mould is adopted. The dynamic behaviour of the fluid in the liquid bridge is governed by incompressible continuing equation, Navier–Stokes equation, and energy equation under the associated initial and boundary conditions.

For convenience, the height $L$ of the liquid bridge is adopted as the characteristic length. The typical velocity $U_c = |\partial\sigma/\partial T'| = \Delta T'/(\rho\nu)$ is introduced from the balance of the tangential shear stresses at the free surface. $\Delta T' = T_2' - T_1'$ is the typical temperature which is the applied temperature difference between the top and the bottom rods. The dimensionless quantities may be defined as follows:

Mail address: H. Tang, Z. M. Tang, W. R. Hu, Institute of Mechanics, Chinese Academy of Sciences, Beijing 100080, P.R. China. G. Chen, B. Roux, Institut de Mecanique des Fluides, 1, rue Honnorat, F-13003 Marseille, France.
Paper submitted: January 31, 1996
Submission of final revised version: May 27, 1996
Paper accepted: June 14, 1996

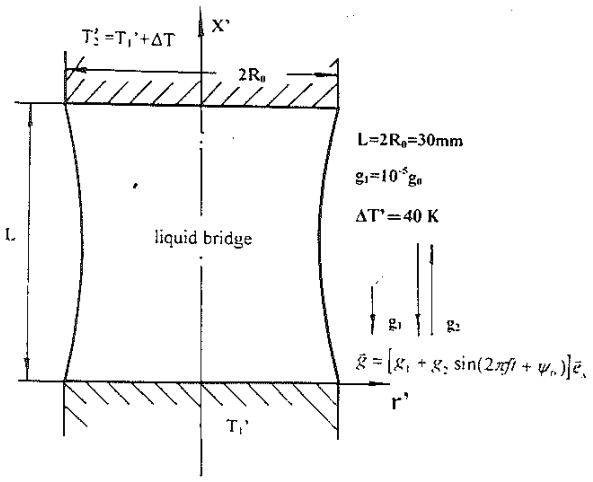


*Fig. 1. Scheme of the liquid bridge*

$$x = \frac{x'}{L},$$

$$y = \frac{r'}{L},$$

$$t = \frac{t' U_r}{L},$$

$$U_r = \frac{|\partial\sigma/\partial T'|}{\rho\nu},$$

$$u = \frac{u'}{U_r},$$

$$v = \frac{v'}{U_r},$$

$$T = \frac{T' - T_1'}{\Delta T'},$$

$$Bo = \frac{g_1 \rho L^2}{\sigma},$$

$$Re = \frac{U_r L}{\nu},$$

$$Ma = \frac{U_r L}{k},$$

$$Gr = \frac{g_1 \beta \Delta T' L^3}{\nu^2},$$

where superscript prime expresses a dimensional quantity (for example $(u', 0, v')$ is the dimensional velocity vector). $\sigma$, $\beta$, $\nu$, $k$, $\partial\sigma/\partial T'$, and $g_1$ are, respectively, the surface tension, thermal expansion coefficient, kinematic viscosity, thermal conductivity coefficient, differentiation of surface-tension with respect to temperature, and the steady part of gravity. The non-dimensional parameter $Bo$ is the static Bond number, $Gr$ the Grashof number, $Re$ the Reynolds number based on the typical velocity $U_r$, and $Pr = \nu/k$ the Prandtl number. Marangoni number, Reynolds number and Prandtl number are connected by the relation $Ma = Re \cdot Pr$.

The Boussinesq approximation for incompressible fluid is used. Navier–Stokes equation and energy equation described by dimensionless vorticity $\omega$, stream function $\psi$ and temperature $T$ are applied for the convection and heat transfer processes in the liquid bridge.

We introduce, respectively, the stream function $\psi$ and vorticity $\omega$, in non-dimensional cylindrical coordinates, as follows:

$$u = \frac{\partial(y\psi)}{y\,\partial y}, \quad v = -\frac{\partial\psi}{\partial x}, \quad \omega = 0, \tag{1}$$

$$\omega = \frac{\partial v}{\partial x} - \frac{\partial u}{\partial y}. \tag{2}$$

Then, the dimensionless equations for $\psi$, $\omega$, and temperature $T$ may be written as follows:

$$\frac{\partial^2\psi}{\partial x^2} + \frac{\partial^2\psi}{\partial y^2} + \frac{\partial\psi}{y\,\partial y} - \frac{\psi}{y^2} = -\omega, \tag{3}$$

$$R_s\left(\frac{\partial\omega}{\partial t} + \frac{\partial(y\psi)}{y\,\partial y}\frac{\partial\omega}{\partial x} - \frac{\partial\psi}{\partial x}\frac{\partial\omega}{\partial y} + \frac{\omega}{y}\frac{\partial\psi}{\partial x}\right) = \frac{\partial^2\omega}{\partial x^2} + \frac{\partial^2\omega}{\partial y^2} + \frac{\partial\omega}{y\,\partial y} - \frac{\omega}{y^2} - \frac{Gr\cdot(1+\alpha)}{R_s}\frac{\partial T}{\partial y}, \tag{4}$$

$$Ma\cdot\left(\frac{\partial T}{\partial t} - \frac{\partial\psi}{\partial x}\frac{\partial T}{\partial y} + \frac{1}{y}\frac{\partial(y\psi)}{\partial y}\frac{\partial T}{\partial x}\right) = \frac{\partial^2 T}{\partial x^2} + \frac{\partial^2 T}{\partial y^2} + \frac{1}{y}\frac{\partial T}{\partial y}. \tag{5}$$

The boundary conditions are summarized as follows:

$$\psi(y, 0, t) = \psi(y, 1, t) = \psi(0, x, t) = 0 \tag{6}$$

$$\frac{\partial\psi(H(x), x, t)}{\partial x} = -\left(\frac{\partial H}{\partial t} + \left(\frac{\partial\psi}{\partial y} + \frac{\psi}{y}\right)\frac{\partial H}{\partial x}\right), \tag{7}$$

$$\omega(y, 0, t) = \omega(y, 1, t) = \frac{2(\psi_{w+1} - \psi_w)}{\Delta x^2}, \tag{8}$$

$$\omega|_{x=H(x)} = \frac{2H}{(1-H_x^2)}\left(2\frac{\partial v}{\partial y} + \frac{v}{y}\right) + 2v_x + \frac{(1+H_x^2)}{(1-H_x^2)}\frac{dT}{dS}, \tag{9}$$

$$T(y, 0, t) = 0. \quad T(y, 1, t) = 1, \quad \frac{\partial T(H(x), x, t)}{\partial n} = 0. \tag{10}$$

$$2\mu H_x(u_y - v_x) + \mu(1 - H_x^2)(u_y + v_x) = \sigma_T(T_x + H_x T_y)(1 + H_x^2)^{1/2}, \tag{11}$$

$$(P_x - P) + 2\mu\frac{1}{1+H_x^2}(H_x^2 u_x - H_x(u_y + v_x) + v_y) = \sigma\left(\frac{H_{xx}}{(1+H_x^2)^{3/2}} - \frac{1}{H_x(1+H_x^2)^{1/2}}\right), \tag{12}$$

where the subscripts $x$ and $y$ denote differentiation with respect to $x$ and $y$. $\psi_{w+1}$ and $\psi_w$ are respectively the stream function values at the distance $\Delta x$ from the rods. The equation of free surface is described as

$$y = H(x). \tag{13}$$

Eqs. (11) and (12) represent the force balance condition along the free surface. In eq. (9), the vorticity at the free surface is given by the equilibrium condition of tangential stresses (eq. (11)). Then, the problem is reduced to solve eqs. (3)–(5) under boundary conditions (6)–(12) for certain parameter values.

## 3 Numerical Simulation

In the present problem the direct simulation of equations and boundaries mentioned above is carried out, the type of basic equations is convection-diffusion under microgravity condition. The hybrid method of fractional steps with the modified characteristic procedure for convection operator and the lumping finite element method for diffusion term is used in the present programme. The liquid bridge is divided into 306 triangular elements with 209 nodes. The linear interpolation and Galerkin technique are used for the discretion of the differential equation.

The height $L$ and the diameter $2R_0$ of the liquid bridge are adopted as 30 mm and 30 mm respectively, the temperature difference $\Delta T'$ is 40 K. The liquid bridge volume is an important factor influencing the half floating zone convection. The ratio of the liquid bridge volume $V_1$ to the cylinder volume $V_0$ is fixed in the present paper and adopted as $V_1/V_0 = 0.8$. The body force is represented in the form

$$g = g_1 + g_2 \sin(2\pi ft + \phi_0), \quad \alpha(t) = \frac{g_2}{g_1} \sin(2\pi ft + \Phi_0), \quad (14)$$

where $g_1$ is a steady axial acceleration acting along the negative $z$-direction under microgravity. $g_2$ is the amplitude of the applied acceleration.

The steady solutions of $(\psi_0, \omega_0, T_0)$ corresponding to $g_1 = 10^{-5} g_0$ and $g_2 = 0$ (before subject to periodical vibrations) were adopted as the initial value, where $g_0$ is the steady earth gravitational acceleration. Fig. 2 shows the initial isotherms and streamlines in steady state.

The periodical vibration $g_2 \sin(2\pi ft + \Phi_0)$ is applied afterwards, where $g_2 = 10^{-3} g_0$. The system response to the periodical vibration was studied after the time evolution. For unsteady calculation of the periodical vibration, the size of time step was determined by stability condition. In this programme, each non-dimensional time equals to 0.119 s (real time) and every time step is about 0.013 non-dimensional time. The free surface shape which is calculated for every 5 time steps is obtained by the normal stress equilibrium condition.

Using the linear interpolation method, 3 fixed points $(p1, p2, p3)$ were chosen in the liquid bridge to illustrate the temperature response. Point $p4$ is on the free surface $(x = 0.17)$ and its position will change during the computational process.

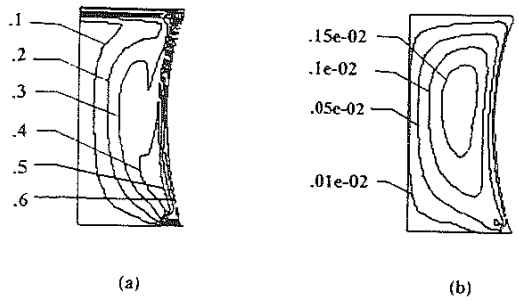


*Fig. 2. Steady state isotherms (a) and streamlines (b) for $g_1 = 10^{-5} g_0$, $g_2 = 0$, $L = 30\,mm$, $R_0 = 15\,mm$, and $\Delta T' = 40\,K$*

Fig. 3 shows the evolution of maximum stream functions at different vibration frequency (a) $f = 1$ Hz, (b) $f = 2$ Hz, (c) $f = 4$ Hz, (d) $f = 10$ Hz. It shows that in addition to its periodical oscillation as response to the applied vibration, the maximum stream function will decrease and attain a steady value after some elapsed time. The steady value will depend on the frequency of the applied vibration and be affected by the frequency adversely (lower with higher frequency). The characteristic time for the maximum stream function to reach a steady value also depends on the vibration frequency, for example, the characteristic time is about 40 on the non-dimensional time scale for $f = 10$ Hz and 80 for $f = 2$ Hz.

Fig. 4 shows the temperature response of the fixed points $(p1, p2, p3)$ and the free surface point $p4$ as a function of the non-dimensional time with different vibration frequency and same vibration amplitude $10^{-3} g_0$, where (a) $f = 1$ Hz, (b) $f = 2$ Hz, (c) $f = 4$ Hz, (d) $f = 10$ Hz, (e) $f = 30$ Hz. It can be seen that the temperature oscillates as response to the applied vibration. The mean part of the temperature response will gradually increase and ultimately attain a steady value after an elapsed time. It seems that this steady value and the elapsed time depend on the vibration frequency. When the frequency is higher, the elapsed time is less and the steady value is higher. For example, the elapsed time is 40 on the non-dimensional time scale for $f = 10$ Hz and 80 for $f = 2$ Hz. These elapsed times for temperature response are almost the same as those for the maximum stream function; it seems that the flow and the temperature field attain their harmonic oscillation state simultaneously. Here we can also find that the frequency of the temperature response equals to the vibration frequency, but the phase of the temperature response opposes the phase of vibration. Point $p4$ changes during the computational process. It may be the reason why its temperature does not have significant fluctuation.

Fig. 5 shows the relation between the mean part of the temperature oscillation and the frequency $f$ of the applied vibration. We can see that the mean part of the temperature response not only increases with vibration environment but also increases with the increasing of the applied frequency at a fixed vibration amplitude.

Fig. 6 shows the evolution of isotherms (a–d) and streamlines (e–h) during 1 period (1 s) for $f = 1$ Hz and $g_2 = 10^{-3} g_0$ at the non-dimensional time $t = 84$. At this time, the flow and the temperature field is oscillating harmonically with the applied periodical vibration. Here we can see that the structure of the flow pattern and the thermal field are significantly changed compared with the steady state condition. The vortex cell becomes small and is closer to the hot rod. The motion of the fluid is retarded and the intensity of the flow is smaller. Corresponding to the change of the flow pattern, the temperature field grows smoothly. In fact, as the intensity of the flow decreases, the thermal transfer in the liquid bridge goes down, maybe it is the reason why the temperature gradient nearby the free surface is attenuated.

Fig. 7 shows the isotherm difference (a–d) and streamline (e–h) difference which are the results of isotherms and streamlines (fig. 3) in unsteady state condition subtracting

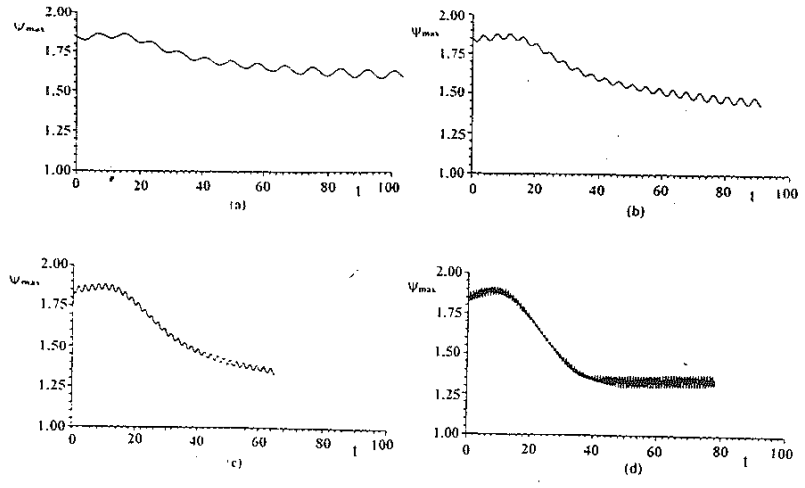


*Fig. 3. Evolution of maximum stream functions as a function of non-dimensional time (a) $f = 1$ Hz, (b) $f = 2$ Hz, (c) $f = 4$ Hz, (d) $f = 10$ Hz*

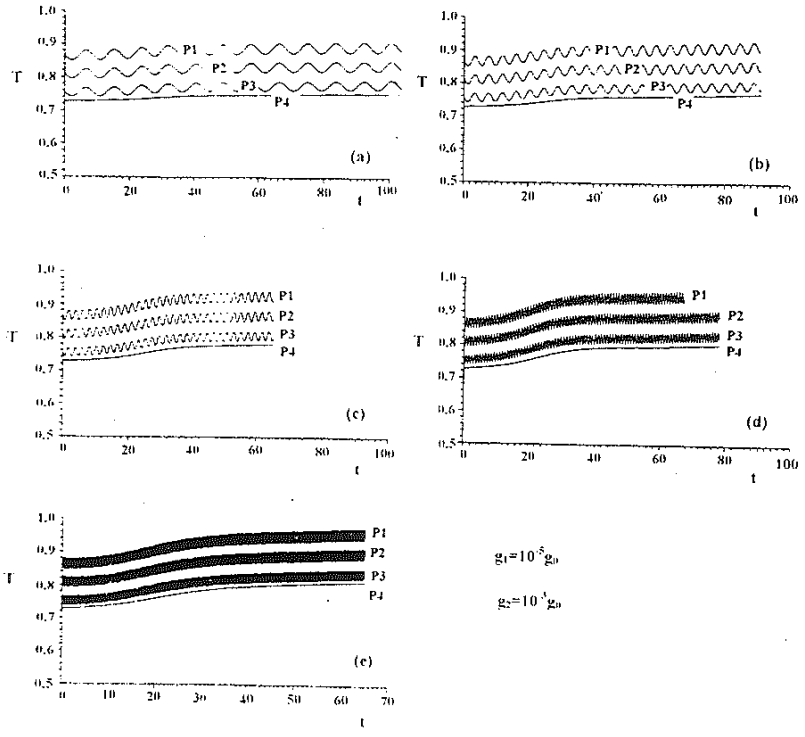


*Fig. 4. Temperature response of the fixed points (p1, p2, p3) and the free surface point p4 at $g_1 = 10^{-5} g_0$, $g_2 = 10^{-3} g_0$. (a) $f = 1$ Hz, (b) $f = 2$ Hz, (c) $f =$ Hz, (d) $f = 10$ Hz, (e) $f = 30$ Hz*

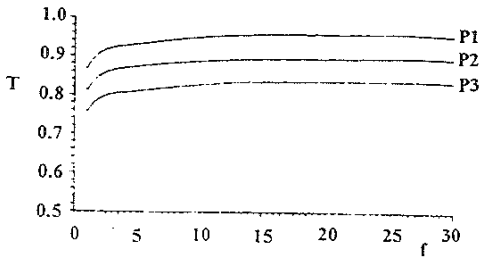


*Fig. 5. The relation between the mean part of the temperature response and the frequency f of the applied vibration*

that in the steady state. It seems that the change of the temperature field mainly happens nearby the free surface whose temperature gradient is higher. Here we can also see that the slight periodical changes of the isotherms and the streamlines have the same frequency as the applied acceleration.

Figs. 8 and 9 show the isotherms, streamlines (fig. 8) and the corresponding isotherm difference, as well as streamline difference (fig. 9) during 1 period (1 s) at the non-dimensional time $t = 84$, where the amplitude of vibration increases to $g_2 = 5 \cdot 10^{-3} g_0$. Here we can see that the isotherms become

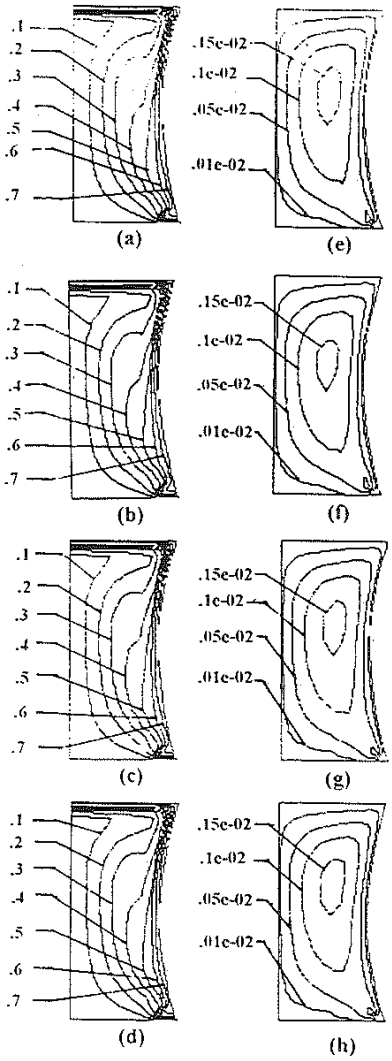


*Fig. 6. Isotherms (a–d) and streamlines (e–h) during 1 period (1 s) time sequence for $f = 1$ Hz, $g_2 = 10^{-3} g_0$. (a, e): $t' = t_0$, (b, f): $t' = t_0 + 0.25$ s, (c, g): $t' = t_0 + 0.50$ s, (e, h): $t' = t_0 + 0.75$ s*

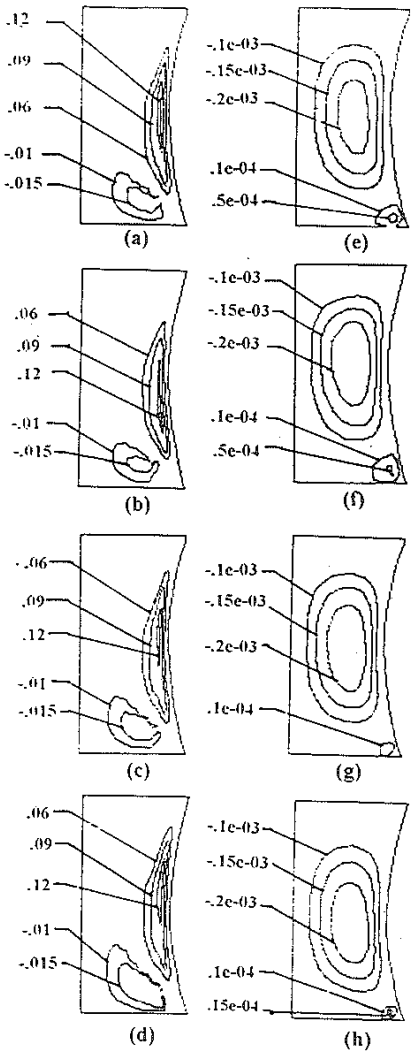


*Fig. 7. Isotherm difference (a–d) and streamline difference (e–h) obtained by subtracting the steady state from the unsteady state in 1 period (1 s) time sequence. (a, e): $t' = t_0$, (b, f): $t' = t_0 + 0.25$ s, (c, g): $t' = t_0 + 0.50$ s, (e, h): $t' = t_0 - 0.75$ s*

smoother and the intensity of the flow tends to be lower when the amplitude of vibration increases.

Fig. 10 shows the free surface configuration at (a) $g_2 = 10^{-3} g_0$ and (b) $g_2 = 5 \cdot 10^{-3} g_0$. We can see that the magnitude of the free surface change will increase with increasing vibration. At $g_2 = 10^{-3} g_0$, the ratio of the maximum free surface change $\Delta H_{max}$ to radius $R_0$ is 1.6 %. When the vibration $g_2$ is increased to $5 \cdot 10^{-3} g_0$, $\Delta H_{max}/R_0$ is 7.8 %.

Fig. 11 shows the variation of 2 fixed points (a) $x = 0.17$ and (b) $x = 0.83$ at the free surface in response to the vibration. It seems that the frequency of the free surface response tends to the frequency of the applied acceleration (for $g_2 = 5 \cdot 10^{-3} g_0$).

## 4 Conclusion and Discussion

This paper studies the influence of gravity vibration on thermocapillary convection numerically; and the deformable free surface is taken into account. A variable grid with time is used successfully. The numerical programme is applied firstly to calculate the thermocapillary convection problem, which has an analytical solution, and the numerical results agree well with the analytical one. The program has also checked with other programs, where similar conclusions were obtained.

The present calculation shows that in addition to its periodical oscillation as response to the applied vibration, the stream function will gradually decay and reach a lower

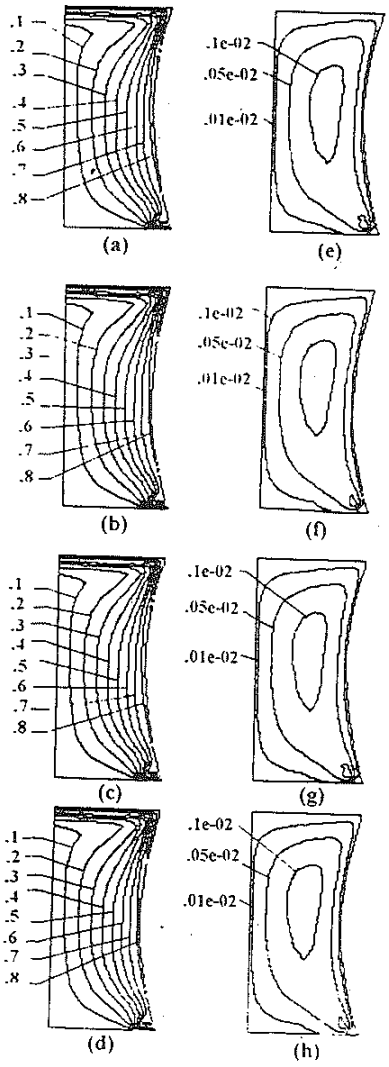


*Fig. 8. Isotherms (a–d) and streamlines (e–h) during 1 period (1 s) for $f = 1$ Hz and $g_z = 5 \cdot 10^{-5} g_0$. (a, e): $t' = t_0$, (b, f): $t' = t_0 + 0.25$ s, (c, g): $t' = t_0 + 0.50$ s, (e, h): $t' = t_0 + 0.75$ s*

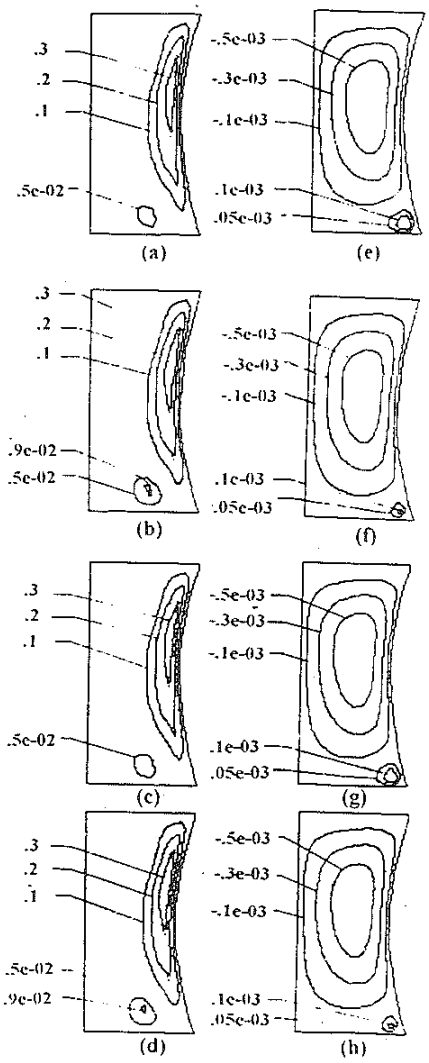


*Fig. 9. Isotherm difference (a–d) and streamline difference (e–h) corresponding to fig. 7. (a, e): $t' = t_0$, (b, f): $t' = t_0 + 0.25$ s, (c, g): $t' = t_0 + 0.50$ s, (e, h): $t' = t_0 + 0.75$ s*

steady value after an elapsed time. This elapsed time will decrease as the vibration frequency is higher. For example, when the frequency increases from 2 Hz to 10 Hz, the elapsed non-dimensional time will decrease from 80 to 40. The mean part of the temperature response has a little rise in the vibration environment, it will keep on a higher steady value after the characteristic time.

The intensity of the flow is lower and the flow is retarded, the temperature distribution is smoother. As the amplitude of the vibration increases, such modulated action on the flow and the temperature field tend to be more obvious.

The results of our simulation are interesting because when the vibration frequency increases, the amplitude of the time varying part of the temperature response keeps almost constant. At the same time, the magnitude of the free surface change is not sensitive to increasing vibration frequency. It means that the effects of surface tension keeps balance against total pressure difference. The shape of the free surface is decided mainly by the pressure difference across the surface. No matter how the pressure is, the response of the free surface is very quick.

It has been shown by *Briskman*'s work [4] that vibrations increase efficiently the Marangoni stability, and that the amplitude of velocity decreases with increased vibrational parameter. These results are qualitatively consistent with ours and give the possibilities of vibrational controlling of thermocapillary convection.

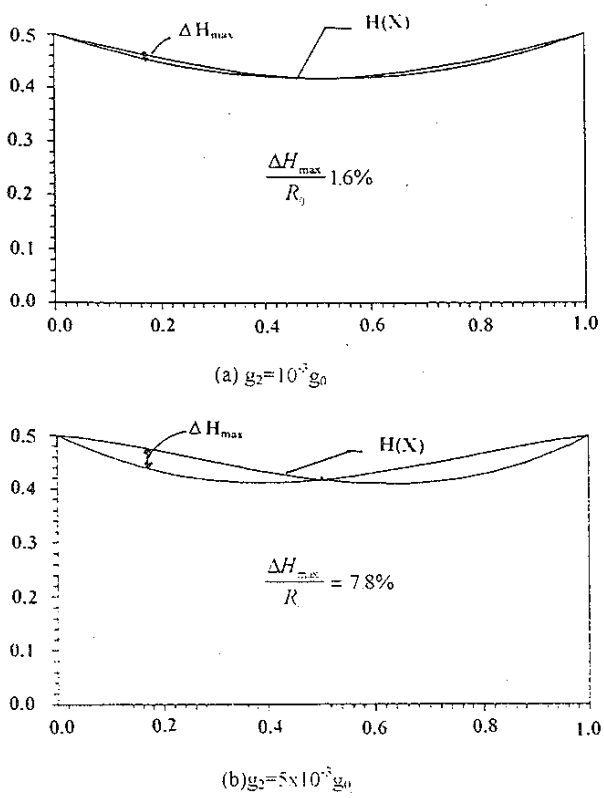


*Fig. 10. Free surface configuration at amplitude of (a) $g_2 = 10^{-3} g_0$ and (b) $g_2 = 5 \cdot 10^{-3} g_0$*

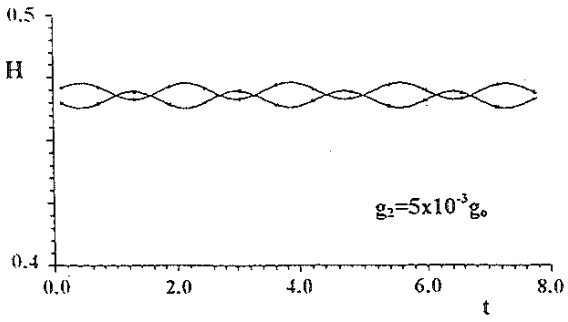


*Fig. 11. Variation of 2 fixed free surface points. (a) $x = 0.17$, (b) $x = 0.83$ in response to vibration for $g_2 = 5 \cdot 10^{-3} g_0$*

## References


1 *Monti, R., Langbein, D., Favier, J. J.:* Influence of Residual Acceleration of Fluid Physics and Material Science Experiment; in: Fluid Sciences and Material Sciences in Space. *H. U. Walter* (ed.). Springer Verlag (1987)

2 *Alexander, J. I. D.:* Low-Gravity Experiment Sensitivity to Residual Acceleration – A Review. Microgravity sci. technol., vol. 3, p. 52 (1990)

3 *Polezhaev, V. I.:* Convection Process in Weightlessness. Science (1991) (in Russian)

4 *Briskman, V. A.:* Vibrational Thermocapillary Convection and Stability. Proc. Int. Conf. Hydromechanics and Heat/Mass Transfer in Microgravity, Perm (1991)

5 *Kamotani, Y., Prassad, A., Ostrach, S.:* Thermal Convection in an Enclosure Due to Vibrations Aboard Spacecraft. AIAA Journal, vol. 19, p. 511 (1981)

6 *Monti, R., Savino, R.:* A New Approach to *g*-jitter Tolerability for Fluid and Material Science Experiments. Proc. 45th IAF-Congr., Jerusalem, IAF-94-J.5., p. 266 (1994)

7 *Alexander, J. I. D., Amiroudine, S., Ouazzani, J., Rosenberger, F.:* Analysis of the Low Gravity Tolerance of Bridgman–Stockbarger Crystal Growth – Part II: Transient and Periodic Acceleration. J. Crystal Growth, vol. 113, p. 21 (1991)

8 *Favier, J. J., Garandet, J. P., Rouzaud, A., Camel, D.:* Mass Transport Phenomena during Solidification in Microgravity – Preliminary Results of the First MEPHISTO Flight Experiment. J. Crystal-Growth, vol. 140, p. 237 (1994)

9 *Tang, H., Zao, Zh., Liu, F., Hu, W. R.:* Effects of *g*-jitter on the Critical Marangoni Number. Microgravity sci. technol., vol. 7, p. 137 (1994)

10 *Tang, H., Liu, F., Hu, W. R.: g*-jitter Effects on Half Floating Zone Convection in Intermediate Frequency Range. Microgravity sci. technol., vol. 8, p. 10 (1995)

11 *Tang, H., Hu, W. R.:* Effects of High Frequency Vibration on Critical Marangoni Number. Advances in Space Research, Vol. 16, p. 71 (1995)